

Computational Investigations on Thin Film Layers using SOI Grating Structures

Nosheen Memon ^{#1}, Muhammad Rafique Naich ^{*2}, Agha Zafarullah Pathan ^{*3}, Baqir Ali Mirjat ^{#4}

[#]Visiting Lecturer & Electronics, Electrical Department & BBSUTSD
Khairpur, Pakistan

^{*}Assistant Professor, Professor & Electrical Department & MUET (SZAB)
Jamshoro, Pakistan

Abstract

This paper illustrates the physical parameters of thin-film layered systems for solar cell technology adopting the Finite Difference Time Domain (FDTD) computational method. The efficiency of the solar cell can increase by improving light absorption content. In this regard, to extract the maximum energy from the sun, the authors studied the Radiative thermal properties of thin-film and including the tapered grating structure of Silicon material on the surface of silicon substrates to enhance its light absorption efficiency. To understand the phenomenon of grating structures, anti-Reflective Silicon on Insulator (SOI) triangular and square grating structures were simulated on the planar waveguides' facets. Results from simulations explain that triangular grating structures provided duction in reflectance when the gradient index's length increased. Power transmittance in triangular and square grating was higher in visible and infra-red regions, respectively. The transmittance parameters, electric field, and Poynting vectors were calculated for given systems, and it is observed that the grating structures significantly modify the absorption efficiency by evenly distributing the photonic energy of lighting the layered thin films. These results can further be extrapolated on an experimental basis to fabricate efficient CZTS-TFSCs for practical applications in the field of solar energy.

Keywords — Absorption, FDTD, Reflectance, Power

I. INTRODUCTION

In the modern era of energy technology, solar energy is one of the most prominent alternative energy sources. Among renewable energies, solar energy is an affable environment source of energy because it does not require fossil fuels responsible for carbon dioxide (CO₂) production or, arguably, nuclear power. The increased industrial growth in solar technology is a sign of its reliability [1].

Regarding the limits of the solar energy extraction light incident on the solar cell, the first key feature is the amount of incident light absorbed (emitting from the solar system) within the device at multiple quantum well regions (if available) or depletion region (p-n junction) or defects within the silicon

semiconductor crystal structure [2]. The p-n junction region (depletion region) produces light inside the diode, and care must be taken for this aspect. As the generated photon carries an energy that matches the band-gap energy of the light-generating, p-n junction region (depletion region) can quickly absorb photons, and it can be at a fast rate [3], [4]. According to the structure, solar cells are categorized as thin-film or bulk solar cells. The thin-film solar cells such as Cu(In, Ga)Se₂(CIGS), CdTe, and CuInSe₂(CIS), have high power conversion efficiency and also high absorption coefficient[5], [6].

A new and efficient approach to solar cell technology is the Cu₂ZnSnS₄ (CZTS), which is the most likely alternative technique. CZTS solar cell technology. It has swept away all the limitations of previously introduced thin-film solar cell techniques and has provided a way to achieve high absorption efficiency [7], [8]. In previous works, the synthesis of CZTS thin films using various vacuum and non-vacuum techniques have been reported [9], [10]. Recently, a new approach based on analytical modeling and Particle Swarm Optimization (PSO) to determine the optimal band-gap profile of the amended CZTS absorber layer to achieve efficiency upto16% to previous CZTS solar cells [11]. Authors in [12] worked on CIGS solar cells and introduced an absorber layer in CIGS-TFSC. Double grading Ga/(Ga+In) provided in CIGS solar cells increase the absorption efficiency in the near-infrared wavelength range. Similarly, authors in [13] proposed micro-crystalline silicon thin-film solar cells; they introduced cadmium-sulfide (CdS) as an n-type buffer layer and light trapping mechanism. Consequently, the efficiency of 9% was observed under global AM 1.5 conditions. Moreover, it is revealed by the study [14] that the optimized physical parameters of metal nanoparticles can enhance the optical and electrical activity of a plasmonic solar cell that is dispersed periodically by using a-Si substrate periods of 2 μm. Furthermore, the authors describe previous reports that represent the presence of potassium, they discussed in detail, and by the additional work upon CIGS mini-modules, achieving efficiency up to almost 19%. [15].

The studies above suggested that CZTS solar cell yields the ideal properties of solar photovoltaic due to its energy band gap of 1.4 eV and has a robust absorption coefficient over 10⁴cm⁻¹ [8]. Using the



transparent conductive oxide (TCO) as a window layer is essential and is widely used in optoelectronic devices [16], [17]. However, AZO is a wide direct band-gap (3.3eV) semiconductor and is a promising alternative to ITO as a TCO for optoelectronic devices because of its advantages such as low-cost non-toxicity and excellent chemical and thermal stability [18], [19].

Keeping in mind the statements mentioned above, the authors investigated triangularly and square SOI grating-based CZTS-TFSCs. In this paper, the simulation of SOI gratings on a substrate is designed. Also, reflection graphs are obtained and compared with the previous studies. The incident light wavelength is 1.55 with a normal incident angle having silicon on insulator grating structure with period $k=400\text{nm}$, spacing $d=200\text{nm}$, and width $w=150\text{nm}$. The ARS structure was used as the conical type, and another simulation was performed by changing the structure of ARS structure from conical to square gratings to obtain the higher anti-reflection values between the working wavelength of 0.5 to 1.0 wavelength while keeping grating period, spacing, and width same as with conical grating structure. This work is helpful to understand the phenomenon of grating structures and their effect on light reflection. Using Opti-FDTD software-based operating method, CZTS thin-film solar cell is designed and simulations performed. As a result, various properties of these structures were obtained. This research work covers the reflectance and absorption properties of CZTS thin-film solar cells [20].

II. COMPUTATIONAL DETAILS

The theoretical analysis of the optical characteristics in the CZTS solar cells with triangular and square SOI grating structures was performed by the Finite Difference Time Domain (FDTD) method based on the Opti-FDTD software package [21].

Fig. 1 shows the flowchart, which describes the working principle of FDTD [22].

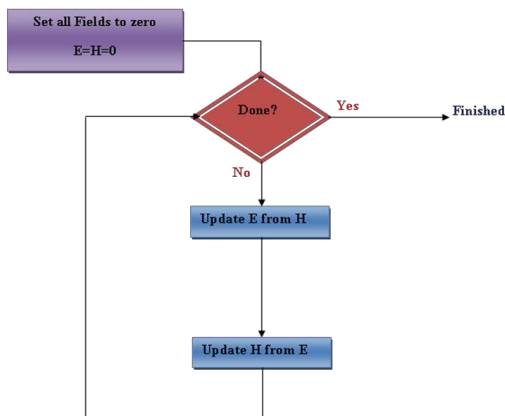


Fig 1: Flow chart for FDTD operating principle

Simulation is designed for different layered structures of CZTS solar cell, including triangular

gratings with a height of $0.3\mu\text{m}$ and 6 grating periods and square gratings with a height of $0.2\mu\text{m}$ and 5 grating periods, a 300nm - 500nm thick AZO TCO layer, a 50nm - 75nm thick intrinsic ZnO layer, a 50nm thick CdS buffer layer, a $1\mu\text{m}$ - $2\mu\text{m}$ thick CZTS absorber layer, a 350nm - 900nm thick Molybdenum (Mo) bottom contact and a glass substrate that comprises the Silicon dioxide (SiO_2) solar cell structure. The cell is a square shape geometry of $4\mu\text{m}\times 3\mu\text{m}$. 2D TE simulations are performed on this design with a Continuous Gaussian Wave (CGW) incident input wave having a wavelength of $1.55\mu\text{m}$ with normal incident angle and a half-width of $0.5\mu\text{m}$. It was assumed that the unpolarized incident light entered from the air into the solar cell. For the constituent materials used in the numerical modeling of a CZTS solar cell, the physical information was employed according to literature that included the IR refractive indices and extinction coefficients For thin-film silicon solar cells and modules incorporating amorphous (a-Si: H) or microcrystalline ($\mu\text{-Si: H}$) silicon as absorber materials, light trapping, i.e., increasing the path length of incoming light, plays a decisive role for device performance [23], [24].

In this simulation, first, the triangular gratings were designed; later on, square structures were placed on the surface TCO layer. Investigations were performed on both the systems; a comparative analysis was also made to determine an efficient absorption model. Table I describes the parameters of the square and triangular grating structure.

TABLE I
Parameters of Square and Triangular gratings

Triangular Grating	Square Grating
Period (K)	400 nm
Spacing (d)	200 nm
Width (w)	150 nm
Height (H)	$0.3\mu\text{m}$
Gratings (n)	6

III. RESULTS AND DISCUSSION

Obtained results and respective analysis on these results is provided as follows;

A. Simulation on triangular grating structure

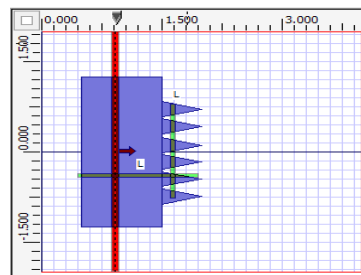
To modify the reflectivity of planar waveguides sub-wavelength grating structure is proposed in different research papers. This technique to alter multilayer structures' reflectance is very important and widely accepted in solar cell technology. Authors of [25] performed rigorous coupled-wave analysis (RCWA) simulation method on sub-wavelength grating (SWG) nanostructures for anti-reflection coatings (ARCs) on $\text{Cu}_2\text{ZnSnS}_4$ (CZTS) solar cells. The analyzed results showed a decrease in reflectance to 1.67%, and efficiency increased to 13.74%. While the simulations were performed using Opti-FDTD software to design the same structure as given in this research paper. The reflectance was

measured and compared again. The results were quite similar, and then a small variation in design was made in which the grating structure was changed from triangular structure to square structure, and also reflectance plot was obtained, which is also shown in Fig. 2(a-c).

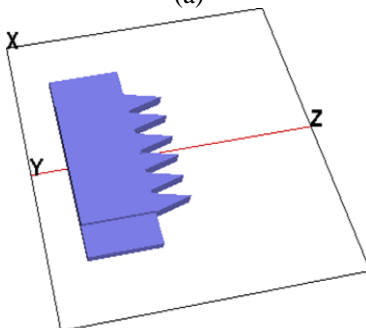
Following Fig. 2(a) explains the design of the triangular grating structure on SOI planar waveguide by using a CAD environment available in Opti- FDTD. The red color thick line shows the input source using continuous Gaussian Wave (CGW) input incident wave and propagating in the z-direction. The small green color lines are observation lines to obtain results of the reflected wave and other parameters.

Whereas Fig. 2(b) shows the extended thin layer made of silicon dioxide, and on the surface of silicon dioxide, gratings of silicon on insulator (SOI) are used. Triangular structures are gratings placed on the silicon's facet on the insulator device, providing an anti-reflective nature to the device.

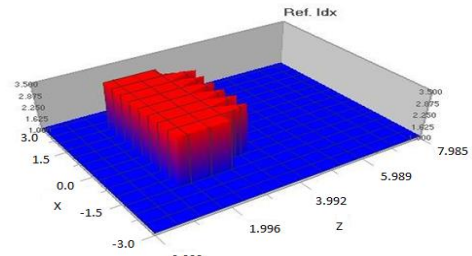
Also, Fig. 2(c) shows the refractive index distribution of the designed structure having material silicon with a refractive index of 3.5 and silicon dioxide with a refractive index of 1.59602. It is clear from the refractive index distribution graph that the gratings are of high valued refractive index. If we notice carefully that the refractive index is not constant in the plot, it is varying from top to bottom because of its dependence on the length of gradient index; this is because the filling factor is not constant as in the case of square grating structure it is exponentially decreasing down concerning change in gradient index.



(a)



(b)

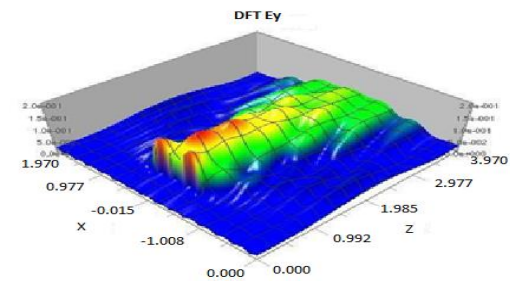


(c)

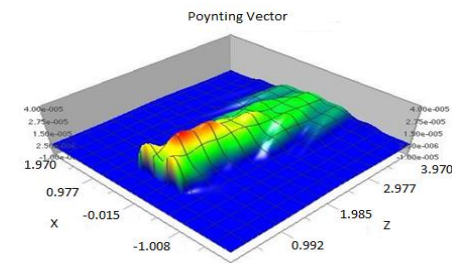
Fig 2: (a) triangular grating structure, (b) thin extended layer, and (c) refractive index.

B. Simulation results on the triangular grating structure

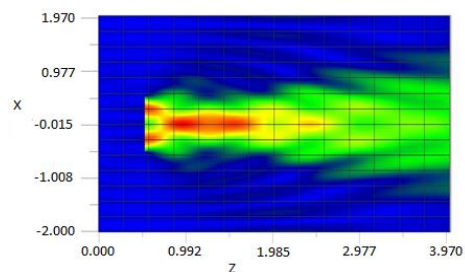
Results obtained after performing 2D simulation on the above design with input wavelength of 1.55 Continuous Gaussian Wave having half-width of 0.5 and normal incident angle of incident wave are shown in Fig. 3(a-c).



(a)



(b)



(c)

Fig 3: (a) Distribution of electric fields, (b) Poynting vector, and (c) E_y color palette plot

As from the above plots, it is clear that due to the AR effect, there is no reflected light in the region left after the mode launching input plane. The above plots are obtained by performing a TE polarization method, so the E_y graph is obtained. TM simulations are also done, and the obtained results were compared.

C. Simulation on square grating structure

In the last reference work, it is stated that instead of triangular grating structures, square gratings could be designed to obtain higher absorption of the electric field inside the structure. To confirm that the same structure was used with a small change of triangular grating structure to square gratings, and results were obtained accordingly. It is observed that when square gratings are used, the light wave propagating through the material is absorbed more, which is shown by the Pointing vector 3D plot. Pointing vector that explains the amount of energy absorbed through the material at different points. The simulation drawing and 3D structure layout, and refractive index distribution, are shown in Fig. 4(a-c).

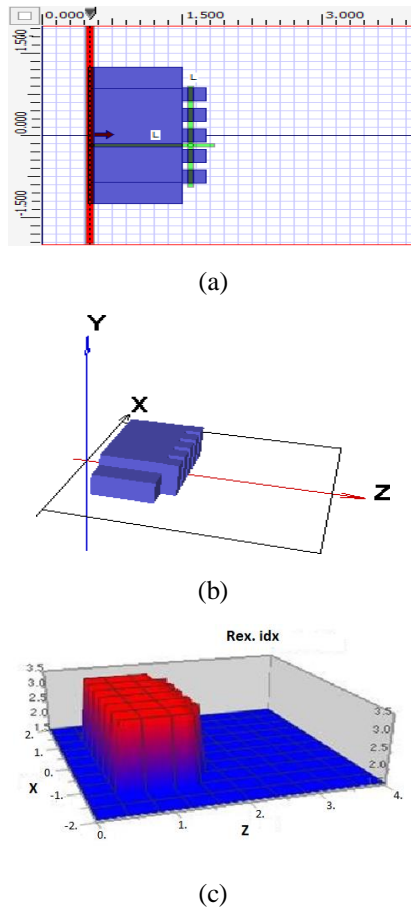


Fig 4: (a) Simulation window, (b) 3D Model, and (c) Refractive index.

D. Simulation results for square grating structure

2D TE simulations are performed on this design with a Continuous Gaussian Wave (CGW) incident input wave having a wavelength of 1.55 with

normal incident angle and half width of 0.5. The results obtained from the simulation are shown below in Fig. 5(a-d).

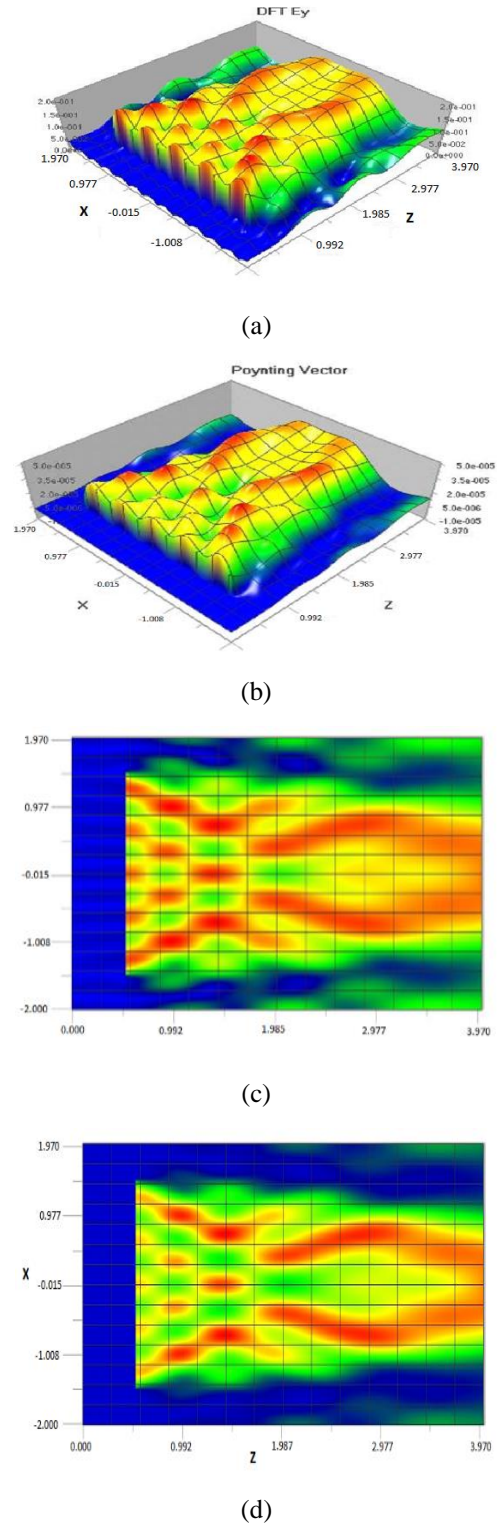


Fig 5: (a) TE simulation results of E_x , (b) Poynting vector 3D plot, (c) Field distribution plot, and (d) Energy distribution plot

E. Power transmittance plot for grating structure

1) Square SOI grating structure

In order to confirm that the square grating structure provides low reflectance and higher absorption of the light wave, a Power Spectrum Plot is obtained by Opti-FDTD, which is showing an increase in power over the increase in wavelength from 0.2 to 1.2 as shown in Fig. 6(a-b).

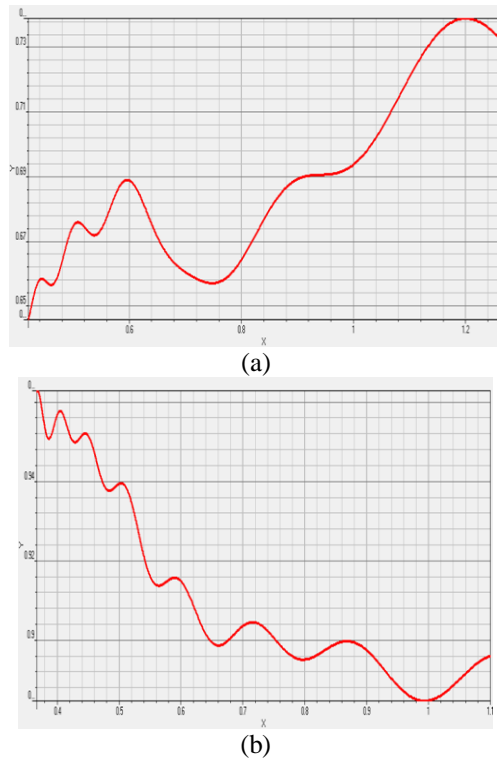


Fig 6: (a) Relative power (Y-axis) vs. gradient index length (X-axis) plot for SGS (b) Relative power (Y-axis) vs. gradient index length (X-axis) plot for TGS

2) Comparison of TGS and SGS

These plots show the Relative Power Transmittance for incident wavelength. We can observe that when the square grating structure is applied on the facets of the planar waveguide, the power transmittance is low during lower wavelengths as in the above plot from 0 to 0.7 the power transmittance is small, and it starts to increase after 0.8 to 1.2 wavelength region.

IV. CONCLUSIONS

In this paper, the authors investigated the thermal radiative properties of CZTS-TFSCs having triangular and square grating structures on its surface. The computational technique adopted for this work is based on the finite difference time domain (FDTD) method employed in the opti-FDTD software package. In triangular grating structure, Anti Reflective characteristics can be obtained as shown in the above plots and 3D field diagrams. It is clear that if the length of the grating index is increasing, the

reflectance decreases. By performing simulation on triangular grating structure, the reflectance values were reduced to 1%. Next, we extended our work to the simulation of the square grating structure. The square gratings were placed at the rear end of the structure, and the source applied at the front end, which caused the higher reflectance at the end of the structure, thus resulting in maximum absorption inside the material instead of transmitting wave with lower absorption. High absorption was gained; thus, power produced in the device was in increasing order because of the increase in the wavelength of the source wave, and as indicated by power diagrams. Comparatively, it can be summarized that triangular grating structures produce high power as the gradient index length increases, whereas square grating structures produce higher power efficiency at lower gradient index length. These results can further be adapted for experimental studies to design and synthesize grating structure CZTS solar cells with higher absorption efficiency than their plan CZTS solar cells.

REFERENCES

- [1] Subash, Suraj, and Masud H. Chowdhury, "High-efficiency carbon nanotube-based solar cells for electronics devices," In Proceedings of the 2009 12th International Symposium on Integrated Circuits, pp. 240-243, 2009.
- [2] Bao, Kui, et al., "Improvement of light extraction from GaN-based thin-film light-emitting diodes by patterning undoped GaN using modified laser lift-off," Applied Physics Letters, vol. 92.14, pp. 141-104, (2008).
- [3] Isabella, Olindo, Janez Krč, and Miro Zeman, "Modulated surface textures for enhanced light trapping in thin-film silicon solar cells," Applied Physics Letters, vol. 97.10, pp. 101-106, (2010).
- [4] Whale, M. D., and Ernest G. Cravalho, "Modeling and performance of microscale thermophotovoltaic energy conversion devices," IEEE Transactions on Energy Conversion, vol. 17.1, pp. 130-142, (2002).
- [5] Jimbo, Kazuo, et al., "Cu₂ZnSnS₄-type thin-film solar cells using abundant materials," Thin solid films, vol. 515.15, pp. 5997-5999, (2007).
- [6] Mitzi, David B., et al., "The path towards a high-performance solution-processed kesterite solar cell," Solar Energy Materials and Solar Cells, vol. 95.6, pp. 1421-1436, (2011).
- [7] Fang, Jin, Hugo Frederich, and Laurent Pilon, "Harvesting nanoscale thermal radiation using pyroelectric materials," Journal of Heat Transfer, vol. 132.9, pp. 092-701, (2010).
- [8] Basu, Soumyadip, and Mathieu Francoeur, "Near-field radiative transfer based thermal rectification using doped silicon," Applied Physics Letters, vol. 98.11, pp. 113-106, (2011).
- [9] Kobayashi, Takeshi, et al., "Investigation of Cu₂ZnSnS₄-based thin-film solar cells using abundant materials," Japanese Journal of Applied Physics, vol. 44.1S, pp. 783, (2005).
- [10] Katagiri, Hironori, et al., "Enhanced conversion efficiencies of Cu₂ZnSnS₄-based thin-film solar cells by using the preferential etching technique," Applied physics express, vol. 1.4, pp. 041-201 (2008).
- [11] Ferhati, H., and F. Djeflal, "Graded band-gap engineering for increased efficiency in CZTS solar cells," Optical Materials, vol. 76, pp. 393-399, (2018).
- [12] Yan, Lingling, et al., "Extending absorption of near-infrared wavelength range for high-efficiency CIGS solar

- cell via adjusting energy band,” *Current Applied Physics*, vol. 18.4, pp. 484-490, (2018).
- [13] Jabeen, Maria, Shyqyri Haxha, and Martin DB Charlton, “Improved efficiency of microcrystalline silicon thin-film solar cells with a wide band-gap CdS buffer layer,” *IEEE Photonics Journal*, vol. 9.6. pp. 1-14, (2017).
- [14] Choudhury, Saniat Ahmed, and Mustafa Habib Chowdhury, “Use of plasmonic metal nanoparticles to increase the light absorption efficiency of thin-film solar cells,” 2016 IEEE International Conference on Sustainable Energy Technologies (ICSET). IEEE, 2016.
- [15] Reinhard, Patrick, et al., “Cu (In, Ga) Se $\times 2$ Thin-Film Solar Cells and Modules—A Boost in Efficiency Due to Potassium,” *IEEE Journal of Photovoltaics*, vol. 5.2, pp. 656-663, (2014).
- [16] Katagiri, Hironori, et al., “Enhanced conversion efficiencies of Cu₂ZnSnS₄-based thin-film solar cells by using the preferential etching technique,” *Applied physics express*, vol. 1.4, pp. 041-201 (2008).
- [17] Pareek, Devendra, K. R. Balasubramaniam, and Pratibha Sharma, “Reaction pathway for synthesis of Cu₂ZnSn(S/Se)₄ via mechano-chemical route and annealing studies,” *Journal of Materials Science: Materials in Electronics*, pp. 28.2, vol. 1199-1210, (2017).
- [18] Leem, J. W., D. H. Joo, and J. S. Yu, “Biomimetic parabola-shaped AZO subwavelength grating structures for efficient anti-reflection of Si-based solar cells,” *Solar energy materials and solar cells*, vol. 95.8, pp. 2221-2227, (2011).
- [19] Kuo, Shou-Yi, et al., “Effects of RF power on the structural, optical and electrical properties of Al-doped zinc oxide films,” *Microelectronics Reliability*, vol. 50.5, pp. 730-733, (2010).
- [20] Basu, Soumyadipta, and Mathieu Francoeur, “Near-field radiative transfer based thermal rectification using doped silicon,” *Applied Physics Letters*, vol. 98.11, pp. 113-106, (2011).
- [21] Li, Z. Q., Y. G. Xiao, and ZM Simon Li, “Modeling of multi-junction solar cells by Crosslight APSYS,” *High and Low Concentration for Solar Electric Applications*, Vol. 6339, International Society for Optics and Photonics, 2006.
- [22] Oloomi, S. A. A., A. Saboonchi, and A. Sedaghat, “Parametric study of nanoscale radiative properties of doped silicon multilayer structures,” *World Applied Sciences Journal*, vol. 8.10, pp. 1200-1204, (2010).
- [23] Müller, Joachim, et al., “TCO and light trapping in silicon thin-film solar cells,” *Solar energy*, vol. 77.6, pp. 917-930, (2004).
- [24] Levchenko, S., et al., “Optical constants of Cu₂ZnSnS₄ bulk crystals,” *Moldavian Journal of the Physical Sciences*, vol. 8.2, pp. 173, (2009).
- [25] Kuo, Shou-Yi, and Ming-Yang Hsieh, “Efficiency enhancement in Cu₂ZnSnS₄ solar cells with subwavelength grating nanostructures,” *Nanoscale*, vol. 6.13, pp. 7553-7559, (2014).
- [26] Nilambar Muduli, J.S.N Achary, “Analysis and Comparison of Liquid Sensing using Silica and BK7 Material PCF by 2D FDTD Method” *SSRG International Journal of Applied Physics* 5.3 (2018): 22-28.